

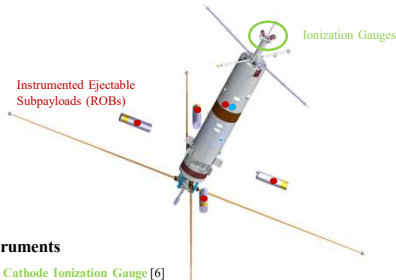
Nathan Graves¹ (gravesn@my.erau.edu) Aroh Barjatya¹ Rob Clayton¹ Henry Valentine¹ Gerald Lehmacher²
(1) Embry-Riddle Aeronautical University, Daytona Beach, FL, United States, (2) Clemson University, Clemson, SC, United States

Abstract

Measurements of aerodynamic drag on objects can be used to determine the density of the medium. The Space and Atmospheric Instrumentation Laboratory at Embry-Riddle Aeronautical University launched a midlatitude sounding rocket named SpEED Demon from Wallops Flight Facility in August 2022. SpEED Demon has a comprehensive suite of instruments for electrodynamic and neutral dynamics measurements. Among these are sensitive low-cost MEMS accelerometers allowing for neutral density measurements up to 100km in altitude. In addition to sensitive accelerometers on the main payload, four ejectable subpayloads also carry an accelerometer providing simultaneous multi-point neutral density measurements, akin to a 'falling cylinder' experiment. The measurements of neutral density via accelerometers will be cross-validated by an ionization gauge onboard the main payload. We present the flight performance and results of this measurement technique from the SpEED Demon launch.

Drag-based Density Measurement Background

Measurements of neutral density in the altitude range of (50-200km) have been a target of sounding rocket missions for a long time. Neutral density measurements have been gathered via the active and passive falling sphere [1][2], neutral mass spectrometers [3], and more recently hot and cold cathode ionization gauges [4]. A recent rocket payload carried a MEMS accelerometer, showing good agreement with an ionization gauge instrument on the same payload up to 80km altitude [5]. MEMS accelerometers continue to improve in cost, size, and sensitivity. Additionally, they require no external interfacing making them easy to integrate into any rocket mission. Extracting neutral density information from accelerometer measurements is therefore worthwhile.



Instruments

Cold Cathode Ionization Gauge [6]

Pfeiffer PKR360 x 2
Mounted 45° from axial fore end on the main payload
Measurement range: 7.5e-10 to 750 torr
5kHz measurement frequency
5% Repeatability
Calibrated at Clemson University

ADXL355 [7]

1x Centrally located on main payload, 4x on subpayloads
±2g measurement range
-30 μg resolution
0.25 - 2.5 kHz measurement frequency

Kionix KXR94-2283 [6]

1x Centrally located on main payload
±0.5g measurement range
5kHz measurement frequency
Flight Heritage: MTeX[5]



Main Payload Accelerometer Box



Subpayload PCB

Table 1: Mechanical specifications of the payloads relevant to drag effects on the accelerometers.

Parameter	Main Payload	Subpayload
Acceleration Noise [μg/sqrt(Hz)]	45/25	25
Payload Length [mm]	2200	335
Payload Diameter [mm]	450	84
Ballistic Coefficient [kg/m ²]	85-550	40-190
Sampling Rate [kHz]	5/2.5	250

Ionization Gauge Calibration



Figure 1: Image of the calibration setup in SAIL. Test Equity 115A shown on right. Left: Up to 3 Keithley 2450 source meters for simultaneous calibration.

The ionization gauges were calibrated in a two-step process. The voltage output of the PKR360 sensor was calibrated against an MKS Baratron® high accuracy gauge at Clemson University. Three runs were performed for each gauge, involving testing a range of pressures over the expected flight conditions. An additional calibration of the voltage measurement box was performed in the Space and Atmospheric Instrumentation Lab at Embry-Riddle Aeronautical University. Calibrating its counts to voltage conversion over a temperature range of 25°C to 55°C in 10°C steps. The pressure calibration fit is ±20% over the range to 10⁻⁵ Torr.

Ionization Gauge Flight Data

Figure 2 shows the calibrated pressure data from each of the ionization gauges on the main payload. The data are compared against the NRL-MSISE00 model. Due to the ionization gauge being mounted on the nose of the payload that may be moving in the ram direction at supersonic velocities, they will measure an elevated pressure from the background. This can be corrected for by computing a ram factor according to the equation:

$$RF(S) = \sqrt{\frac{T_1}{T_2}} \exp(-S^2) + \sqrt{\pi} S (1 + \text{erf}(S)) \quad (1)$$

$$S = \frac{v \cos(\alpha)}{\sqrt{2kT_1/m}} \quad (2) \quad [5][9]$$

Where α is the angle of attack to the ram direction, T_1 is the neutral temperature, T_2 is the temperature within the gauge, and m is the mean molecular mass.

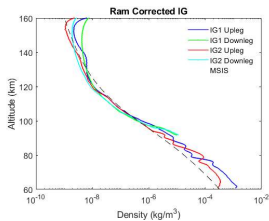


Figure 3: Ram-corrected ionization gauge density data.

Accelerometer Flight Data

$$a_{drag} = C_d \frac{\rho v^2}{2m} A_{proj} \quad (3); \quad \rho = \frac{2m a_{drag}}{C_d A_{proj} v^2} \quad (4)[1]$$

Figure 4 shows the theoretical acceleration due to drag for the subpayload experiment as a function of altitude and relative velocity between the object and the medium. It is assumed that the projected area to ram and drag coefficient is constant. The nominal rocket flight path is shown. The analog and digital accelerometers flown should be capable of resolving density up to 105-110 km, in the best case. More expensive accelerometers are also shown, as future instruments of interest. The MEMS devices are small 9x9mm chips, the IEPE are 2" cylinders.

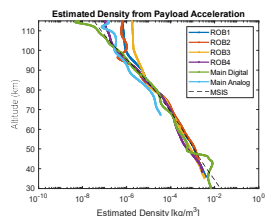


Figure 4: Theoretical acceleration due to drag for subpayloads compared to sensor noise floors. Nominal rocket altitude-velocity trajectory shown in red.

Estimated density, as shown in Figure 5, is computed using Eqn (4). The acceleration due to drag (a_{drag}) is the sensor measurement. For this analysis it is assumed that the entire acceleration magnitude is due to the force of drag. The velocity is derived from GPS measurements. The projected area (A_{proj}) is assumed to be the area of the payloads with the long axis oriented perpendicular to the ram direction (length multiplied by diameter in Table 1). Since the payloads are coning, this is a poor assumption, and the raw acceleration magnitude measurements vary sinusoidally with this changing area. However, computing the signal envelope of the acceleration signal will result in a value close to this maximum area. The drag coefficient (C_d) is applied using published data on circular cylinders in a Reynolds number range of 10-10⁶ [10]. For altitudes above ~80km, transitional flow conditions begin, and free molecular flow modeling should be applied. This is one cause of inaccuracy in the high-altitude data.

Figure 5: Density derived from acceleration measurements on all payloads using Eqn (4). Main is main payload and ROB is subpayload measurement.

Figure 6 shows the acceleration-derived density ratio for each of the instruments. The current assumptions of C_d and projected area are most valid in 80-90km range, which is where the instruments most closely match the model. Above 90km, the continuum flow C_d no longer applies and below 80km, the subpayload angle of attack to the ram is likely to shift. These assumptions must be accounted for in order to draw conclusions about interesting features in the data, like winds or gravity waves.

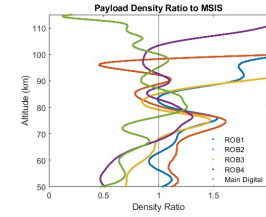


Figure 6: Payload Density Ratio to model.

Improvements

The largest assumption in the current technique is the projected area in the ram direction remains constant. Figure 7 shows that the projected area remains within ±5% for a 30° deviation from the assumed case, however it drops off quickly from there. Increased drag will cause the subpayload long axis to begin aligning to the ram direction as it descends, which is the likely cause of the underestimate shown in Figure 6. Correcting for projected area is possible by developing an attitude solution from other sensors on board the subpayloads.

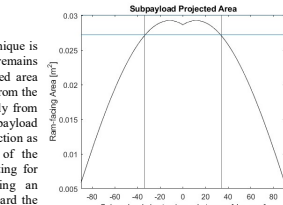


Figure 7: Subpayload projected area calculation, with blue line showing -5% from assumed value.

Applying an attitude solution also allows each axis to make an independent measurement of the drag, as well as resolve accelerations in the geodetic reference frame, to detect winds. Additionally, knowledge of the attitude can improve the artificial noise floor instated by tumbling motion. As seen in Figure 8, some subpayloads have an artificial noise floor when using the envelope technique. An attitude solution should reduce this artificial noise floor.

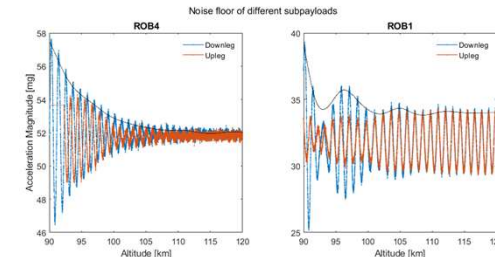


Figure 8: Acceleration magnitude shown in the altitude range where drag acceleration rises above the artificial noise floor, which is worse in some subpayloads.

Takeaways

- The flight performance of a distributed set of accelerometers measuring neutral density drag has been demonstrated up to an altitude of 90-110km. This demonstrates that the 'falling cylinder' technique can be applied in a similar manner as prior 'falling sphere' experiments.
- Development and application of an attitude solution to subpayloads may allow for extending this measurement to 115km for all subpayloads and determination of zonal and meridional winds >20m/s up to an altitude of 60km.
- Using more sensitive, larger, and expensive accelerometers can increase density/wind measurement altitude up to ~150km/110km.
- Direct Simulation Monte-Carlo (DSMC) free molecular flow simulations will be conducted to verify the ionization gauge ram factor on the main payload and acquire a more accurate drag coefficient value for the subpayload at higher altitudes and varying angles of attack.

References

[1] Philbrick, C. R., A. C. Faire, D. H. Fryklund, Measurement of atmospheric density at Kwajalein Atoll, 18 May 1977, *Rep. AFGL TR 78-0058*, 113pp. Air Force Geophysics Lab., 1978 [NTIS AD#054784]
 [2] Schmitt, F.J., Lee, H.S., Michel, W., 1991. The inflatable sphere: A technique for the accurate measurement of middle atmosphere temperatures. *J. Geophys. Res.* 96 (D12), 22673-22682.
 [3] Offermann, D., 1974. Composition variations in the lower thermosphere. *Journal of Geo Research* 79, 4281-4293.
 [4] Lehmacher G.A., Gauden T.M., Larsen M.F., Craven J.D., Multiple neutral density measurements in the lower thermosphere with cold-cathode ionization gauges, *Journal of Atmospheric and Solar-Terrestrial Physics*, Volume 92, 2013, Pages 137-144, ISSN 1364-6826, https://doi.org/10.1016/j.jastp.2012.11.002.
 [5] Lehmacher, G., et al., On the Short-term Variability of Turbulence and Temperature in the Winter Mesosphere. *Annals Geophysicae* 36, 4 (2018). DOI: 10.5194/angeo-36-1099-2018
 [6] Pfeiffer Vacuum, https://www.pfeiffer-vacuum.com/en/
 [7] Kionix, https://www.kionix.com/
 [8] Analog Devices, https://www.analog.com/en/products/adxl355.html
 [9] Patterson, G.N., 1956. *Molecular Flow of Gases*. John Wiley and Sons, New York.
 [10] Heddlson, C. F., et al., 1957. Summary of Drag Coefficients of Various Shaped Cylinders. DTIC ADA395503